Desalination and Water Treatment
www.deswater.com
doi: 10.1080/19443994.2015.1081632

57 (2016) 16435–16444
July

Taylor & Francis
Taylor & Francis Group

Heterogeneous catalytic ozonation by Nano-MgO is better than sole ozonation for metronidazole degradation, toxicity reduction, and biodegradability improvement

Majid Kermani[a], Farshad Bahrami Asl[b,c,*], Mahdi Farzadkia[a], Ali Esrafili[a], Soheila Salahshour Arian[d], Mohammad Khazaei[e], Yousef Dadban Shahamat[f], Dariush Zeynalzadeh[g]

[a]*Department of Environmental Health Engineering, School of Public Health, Iran University of Medical Sciences, Tehran, Iran, Tel. +982186704627; Fax: +982188622707; email: majidkermani@yahoo.com (M. Kermani), Tel. +982188607945; Fax: +982188622707; email: mahdifarzadkia@gmail.com (M. Farzadkia), Tel. +982188607941; Fax: +982188622707; email: a_esrafily@yahoo.com (A. Esrafili)*
[b]*Department of Environmental Health Engineering, School of Public Health, Kermanshah University of Medical Sciences, Kermanshah, Iran, Tel. +984432784378; Fax: +9802188622707; email: farshadfba@gmail.com*
[c]*Department of Environmental Health Engineering, School of Public Health, Hamadan University of Medical Sciences, Hamadan, Iran*
[d]*Student Research Committee, Urmia University of Medical Sciences, Urmia, Iran, Tel. +984432784378; Fax: +9802188622707; email: soheylassa@gmail.com*
[e]*Department of Civil Engineering, Sharif University of Technology, Tehran, Iran, Tel. +982186704627; Fax: +982188622707; email: khazaee_mohammad@yahoo.com*
[f]*Environmental Health Research Center, Golestan University of Medical Sciences, Gorgan, Iran, Tel. +989111789457; Fax: +981732436107; email: ydadban@gmail.com*
[g]*Department of Environmental Health Engineering School of Public Health, Tehran University of Medical Sciences, Tehran, Iran, Tel. +984432784378; Fax: +9802188622707; email: d.zeynalzadeh@yahoo.com*

Received 20 February 2015; Accepted 3 August 2015

ABSTRACT

In the current paper, the removal efficiency of metronidazole (MNZ) using a catalytic ozonation process (COP) in the presence of magnesium oxide nanocrystals, as a catalyst, was investigated in deionized water and compared with a sole ozonation process (SOP). The influence of several operational factors on both removal processes was evaluated: solution pH, MgO dosage, initial MNZ concentration, and reaction time. Biodegradability improvement, mineralization rate, oxidation intermediates, and toxicity were also studied for the COP. The results showed that MgO nanocrystals accelerated MNZ removal compared to the SOP. The optimum pH for both SOP and COP was obtained at 10 and optimum MgO dosage for the COP was determined 0.25 g/L. Under optimum conditions, after 20 min and 35 min, the complete removal of 40 mg/L MNZ solution occurred in COP and SOP, respectively. The COP significantly increased the biological oxygen demand/chemical oxygen demand ratio (from 0.09 to 0.43), caused 93.5% MNZ mineralization, and reduced the toxicity of the MNZ.

*Corresponding author.

Keywords: Bioassay; Catalytic ozonation; MgO nanocrystals; Metronidazole; Ozonation

1. Introduction

A first-generation member of 5-nirtroimidazole drugs derivatives, metronidazole (MNZ) [1,2], is universally used in clinical applications and extensively used for the treatment of infectious diseases caused by protozoa, anaerobic bacteria [2], and some types of periodontal disease [3]. Apart from these applications for humans, MNZ is also abused as an additive in hen and fish feed to eliminate parasites. Thereupon, MNZ is accumulated in animals, fish farm water, and effluents from meat industries [4]. According to the US National Institutes of Health, MNZ induces several inconvenient harmful effects such as headache, gastrointestinal disorders, and hypersensitivity reactions [5]. MNZ is also employed for radiosensitization of hypoxic tumors, being included as a potential human carcinogen by the International Agency for Research on Cancer [5]. Based on the MNZ genotoxicity evaluation using the comet assay, MNZ was found to induce DNA damage in human lymphocytes [6]. Moreover, it has been detected in hospital wastewaters at concentrations of 1.8–9.4 μg/L [1]. As is obvious, the amount of MNZ in the aquatic environment is low. Nevertheless, its continuous input may constitute a potential risk for aquatic and terrestrial organisms [7]. Therefore, it is essential to eliminate this contaminant from water and wastewater in the long term. The chemical and physical characteristics of MNZ are summarized in Table 1 [4,8]. Due to low biodegradability [4], high toxicity [7], high solubility, and resistant character [9], its removal from water and wastewater is difficult. However, it can be removed via methods such as biological methods [10], sorption [11], oxidation processes [12], physical methods [13], application of nanoscale zero-valent iron [4], and advanced oxidation processes (AOPs) [8]. Rivera-Utrilla et al. have studied the removal of nitroimidazole antibiotics from aqueous solution by adsorption/bioadsorption on activated carbon, and he concluded that the presence of microorganisms increases nitroimidazole antibiotics adsorption/bioadsorption on the activated carbon. However, micro-organisms used in wastewater treatment plant cannot degrade these compounds [11], and conventional biological technologies involve long periods of treatment and cannot achieve high removal efficiency [10]. Physical methods, such as flocculation and centrifugal separation, always cause secondary contamination [13]. Using UV radiation for direct photolysis of metronidazole in aqueous solution requires high detention time (8 h) which increases the costs [12]. In adsorption process, contaminants are accumulated and separated from the water, but they were only transformed from one phase to another phase (from the aqueous phase to solid phase) without any degradation [11]. Based on the mentioned researches, it is necessary to search novel and viable technologies for effective removal of metronidazole from water. In recent years, AOPs have been increasingly applied for the removal of various types of organic compounds. Among them, substantial attention has been paid to invest the catalytic ozonation process (COP) as a new method of AOP. In this process, in order to enhance ozone decomposition, forming highly reactive and non-selective hydroxyl radicals, a catalyst is applied. These radicals are able to oxidize the toxic and/or resistant organic compounds into final inorganic products and sometimes convert them to less toxic and more biodegradable intermediates [14]. Thus, using a catalyst along the ozonation increased oxidation rate and decreased reaction time, thereby reducing the required costs. However, the operational variables such as solution pH, temperature, ozone dosage, dose and type of the catalyst, structure of the pollutant(s), and reactor con affect the efficiency of the COP [15]. COPs are often categorized as homogenous and heterogeneous processes. Due to its ease of operation, ability to function at ambient pressure and temperature, low cost, simplicity of catalyst separation, and lack of byproducts, the heterogeneous COP is one of the best methods among recently developed AOPs for treating industrial wastewaters containing persistent

Table 1
Physical and chemical characteristics of MNZ

Molecular formula	$C_6H_9N_3O_3$
Molecular weight (g mol^{-1})	171.2
Water solubility (g L^{-1})	9.5
pK_a	2.55
V_p (Pa)	4.07×10^{-7}
K_H (mol dm^{-3} atm^{-1})	5.92×10^{7}
Melting point (°C)	159–163
Molecular structure	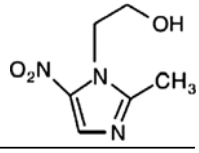

compounds [14]. In recent years, in order to improve COP efficiency in the removal of different contaminants, most efforts have been focused on preparing and perusing new catalysts [15]. Numerous natural and synthetic catalysts such as activated carbon, metal oxides, and metal ions have been applied in COPs for removing various organic compounds [14]. Owing to adsorption capacity, destructive adsorbent, high surface, reactivity, simplicity of production, and lower cost, alkaline earth metal oxides on the nanoscale are very promising materials for catalyst applications. A study conducted by He et al. indicated that using magnesium oxide (MgO) in conjunction with the sole ozonation process (SOP) could accelerate phenol and chemical oxygen demand (COD) removal from solution [16–19]. Moussavi et al. used MgO/GAC along with ozonation for catechol removal [20]. However, SOP and COP efficiencies for MNZ removal and catalytic capacity of MgO nanocrystals in the COP have not been reported for any antibiotic removal. This work focused on the preparation and application of MgO nanocrystals as catalysts in the COP for the removal of MNZ (as a model of nitroimidazole antibiotics), comparing the performance with SOP, a survey of mineralization rate and biodegradability improvement of MNZ solution, identification of oxidation intermediates and bioassay of effluent using Daphnia Magna in COP. The effect of the main operating variables, including pH, reaction time, catalyst dose, and initial MNZ concentration [15], on the COP's performance was compared to the performance of the SOP under the same conditions.

2. Material and methods

2.1. Material and catalyst preparation

Metronidazole and acetonitrile (HPLC grade) were obtained from the Sigma-Aldrich and Samchun (South Korea), respectively. $Mg(NO_3)_2$ and all of the other chemicals and reagents used were of analytical grade and purchased from Merck (Germany). NaH_2PO_4 solution, as the buffer, (50 mM) was used to adjust the pH of experimental solutions. In order to prepare all solutions, distilled water was used. Also, for the credibility of results, all experiments were performed in duplicate. MgO nanocrystals were prepared by a simple calcination as follows: first, the appropriate amount of $Mg(NO_3)_2$ was solved in distilled water; then, the prepared solution was dried at 100˚C for 24 h; and finally, the remaining material was calcinated in the presence of air at 500˚C for 2 h and was crushed [15].

2.2. Experimental apparatus and procedure

2.2.1. Sole and catalytic ozonation process reactor

The sole and catalytic ozonation reactor was a stainless steel cylindrical sparger with a total volume of 1 L, which was fitted with other components including a pure oxygen supply, a flow meter, an ozone generator, an ozone output control system and valves, and tubing. All experiments were performed at a temperature of 22 ± 3˚C under batch reaction, with a solution volume fixed at 500 ml in each run. MgO nanocrystals were used as catalyst along ozonation for MNZ oxidation. Ozone was generated from the pure oxygen by a commercial generator (ARDA, model COG-OM, type 1A) with 5 gO_3/h capacity. The dose of ozone was considered constant at 0.5 g/h. In order to quench and destruct ozone in the off-gas stream of the reactor, KI solution was used.

2.2.2. Biodegradability and mineralization

In order to assess the biodegradability and the mineralization rate of the COP under the optimum condition, the samples were taken from the beginning and end of the reaction and analyzed for biological oxygen demand (BOD_5), COD, and total organic carbon (TOC) tests [21]. Comparison of the BOD_5/COD and TOC for the influent and effluent of the reactor indicated the biodegradability and mineralization changes, respectively.

2.2.3. Oxidation intermediates and toxicity assessment

In order to identify oxidation intermediates under optimum condition, the samples were taken after 10-min ozonation in COP and analyzed by gas chromatography–mass spectrometry (GC–MS). Bioassay of the COP influent and effluent was performed in laboratory scale. First, by the detection range tests, the desired concentrations for bioassay were obtained and 10 numbers of cultured D.Magna were added in each concentration. The mortality percentage was investigated after 24-h and 48-h contact times. Then, lethal concentration 50 (LC_{50}) and toxicity unit (TU) were calculated.

2.3. Analytical methods

The pHzpc of MgO nanocrystals was measured by the pH drift method [22]. Using the scanning electron microscopy images (SEM, HITACHI, S-4160), the morphology of the nanocrystals was investigated. MNZ concentration was determined by high-performance

liquid chromatography (HPLC, CECIL, 4100) equipped with a UV/VIS detector (model, 4200) at 320 nm. A C18ec HPLC column (MACHEREY-NAGEL, 5 μm, 250 × 4.6 mm) was used and the mobile phase was composed of water and acetonitrile (80/20, v/v). The flow was set at 1 ml min^{-1} and injection volumes were 20 μL. A GC–MS system (AGILENT Technologies, 7890A-5975C) was applied for the identification of oxidation intermediates. pH was determined using an electrode (HACH, HQ 40d) and TOC was measured by TOC analyzer (SHIMADZU, TOC-VCSH). The bioassay testing method was based on a standard method referred by Weber CI [23]. Using the Probit analysis in SPSS ver.16, the average mortality rate for experiments was analyzed and LC_{50} was determined. Moreover, the TU was calculated according to Eq. (1). In order to analyze the ozone concentration, the iodometric titration method was used [21].

$$TU = 100/LC_{50} \quad (1)$$

3. Results and discussion

3.1. Catalyst characteristics

The pH-drift experiment results showed a pHzpc value of 12.3 for MgO nanocrystals; this characteristic affects ozone decomposition and performance of process [24]. Fig. 1 shows the pattern of the synthesized MgO, which demonstrates the pure and cubic MgO crystalline particles in the powder [19]. Based on Scherer's equation, the average size of crystals was found to be 73 nm. In order to visualize the surface morphology of the produced MgO, the SEM image shown in Fig. 2 is used; the image demonstrates agglomerated and porous nanocrystals. The surface area of the synthesized powder was investigated by nitrogen adsorption–desorption isotherm (data not shown), which indicated that BET surface area was 137 m^2/g. Based on these results, it is clear that the fabricated powder was composed of mesoporous nanocrystals that had a high specific surface area.

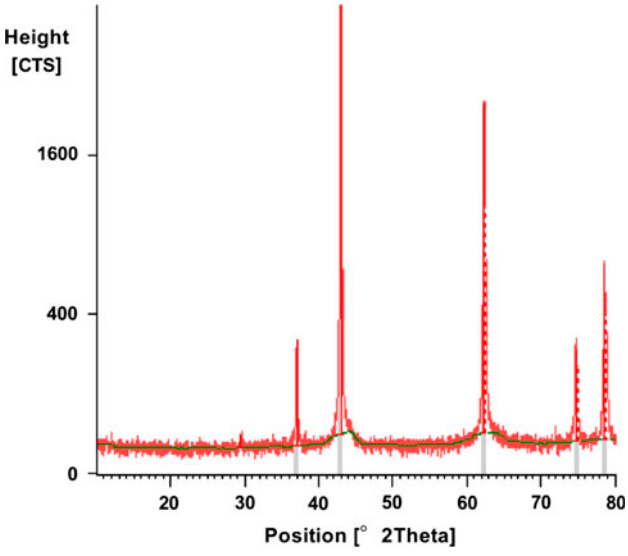

Fig. 1. XRD pattern of the produced powder.

3.2. Effect of initial pH

Since during an oxidation process, solution pH is one of the main factors that affects the contaminant degradation mechanism, it is important to evaluate this parameter on catalytic ozonation of the selected model antibiotic. Therefore, the effect of initial pH of the MNZ solution on MNZ degradation was studied at different pH values ranging from 3 to 12, under constant reaction time and ozone dosing rate in both processes. Removal percentages of MNZ, as a function of initial pH in SOP and COP, have been shown in Fig. 3(a) and (b), respectively.

As seen in Fig. 3(a), the percentage of MNZ removal in SOP at an acidic pH 3 was 91.8%, it decreased to 90.7% at pH 5 and it decreased to 74.1% again with an increase in pH to 7. The high MNZ removal at pH 3 can be explained by direct oxidation of MNZ molecules with ozone, which is best performed at more acidic pH [25]. The removal of MNZ increased for pH values above 7 and reached 97% at pH 10, which is 22.9% higher than that at pH 7. The efficiency of MNZ remained almost unchanged until pH was raised to 12 (97.1%). The rate of ozone decomposition accelerated under alkaline conditions, resulted in the production of more reactive radicals

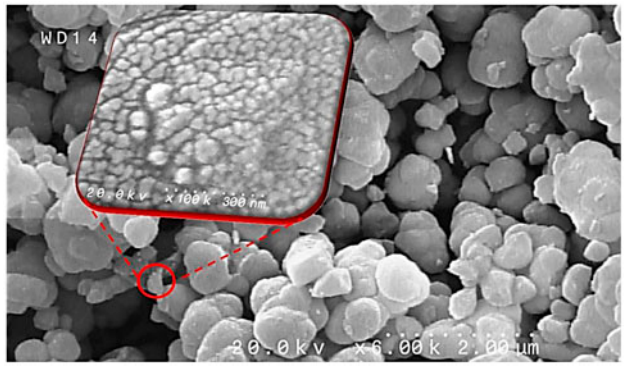

Fig. 2. SEM images of produced MgO nanocrystals.

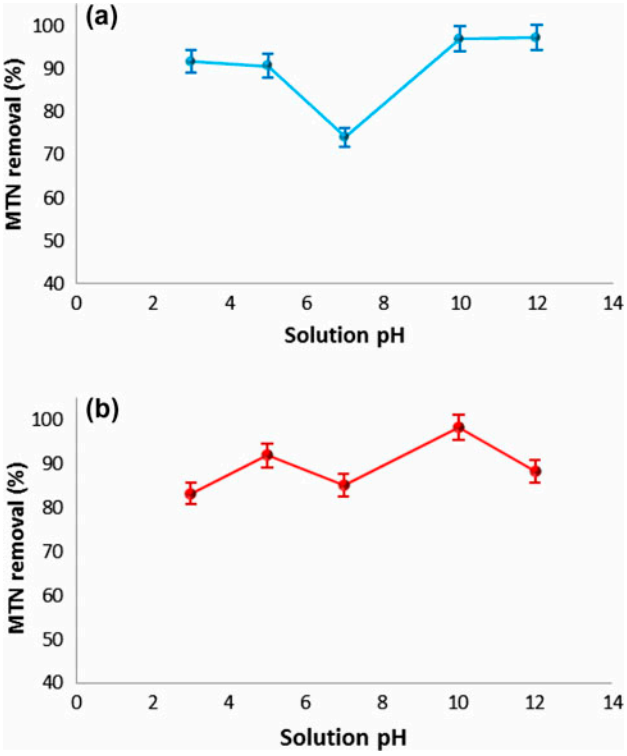

Fig. 3. The effect of initial pH on MNZ removal at: (a) the SOP (MNZ concentration = 40 mg/L, reaction time = 35 min) and (b) the COP (MNZ concentration = 40 mg/L, MgO dosage = 1 g/L, reaction time = 20 min).

[26]. Hence, high degradation of MNZ molecules and high removal of MNZ, at alkaline pHs likely occur by indirect oxidation with radicals. However, some direct oxidation with ozone molecules might also take place. The influence of initial pH on antibiotic ozonation varies in different water backgrounds [27]. The maximum level of antibiotic degradation was reported to occur at a pH level of 10 in hospital wastewater treatment effluent [28]. However, in deionized water, the maximum efficiency of antibiotic removal was reported at both acidic [29] and alkaline pH [30].

Fig. 3(b) presents the efficiency of the COP with MgO nanocrystals. 83.3% of MNZ was removed at pH 3, but contrary to expectation, it increased to 92% when the pH increased to 5. MNZ removal decreased to 85.2% at pH 7. This reveals that at acidic pH, the dominant mechanism was direct oxidation by the ozone molecules, as per the SOP. With an increase inthe pH above 7, the efficiency began to increase and reached a maximum of 98.3% at pH 10 and it decreased to 88.4% when pH increased to 12. Due to the generation of hydroxyl radicals at pH above 10 [31,32] and direct oxidation by ozone molecules under acidic pH, a decrease in the MNZ removal under strong acidic and alkaline condition can be explained by pKa of MNZ (2.55) and pHzpc of MgO nanocrystals (12.3). Based on these two parameters, between solution pH 2.55 and 12.3, MNZ is positively charged and a negative charge is developed on the MgO nanocrystal's surface. Due to zero surface charge of MNZ and catalyst under strong acidic and alkaline conditions, respectively, the affinity of them is restricted to each other. These findings imply that the pH of the MNZ solution acts as an important factor in both SOP and COP. Sui et al. [33] found a negative effect of pH on the catalytic ozonation of ciprofloxacin with carbon nanotube-supported manganese oxides.

In order to confirm the MNZ degradation by the radical oxidation mechanism, tert-butanol was added to the COP [34–37], which resulted in the efficiency. This illustrates that MNZ degradation followed the radical oxidation mechanism. However, direct oxidation of MNZ by ozone molecules might also occur in the COP, as is seen with the SOP. Due to the large specific surface area of the catalyst, the degradation on the surface of catalyst was likely the main mechanism. However, MNZ molecules and intermediates oxidation might be taking place by both radicals and molecular ozone in both bulk solution and on the catalyst surface. According to the results, the maximum MNZ removal in both COP and SOP was at pH 10, thereby this figure was selected as the optimum value in the subsequent catalytic and non-catalytic ozonation experiments.

3.3. Effect of reaction time

Reaction time, as a time required to reach the favorable goals of the process, is one of the important variables in order to design and operate an oxidation process. Hence, after pH optimization, the second phase of this experiment investigated the removal of MNZ by both COP and SOP as a function of reaction time, under the optimum initial pH value of 10. The results have been presented in Fig. 4.

An increase in reaction time increased the removal of MNZ in both processes, although at a higher rate for COP than SOP. For the SOP, the efficiency increased around 62% after 20 min of ozonation. Increasing the reaction time to 35 min led to 98.8% MNZ removal. As observed in Fig. 4, the COP could achieve 92% MNZ removal after a reaction time of only 15 min. The percentage of MNZ removal increased to 99% after 20 min of ozonation. Kinetics of MNZ degradation in both SOP and COP was investigated for zero-order, first-order, pseudo-first-order, second-order, and pseudo-second-order (linearized form type I, II, III, and IV) kinetic models [38]. The

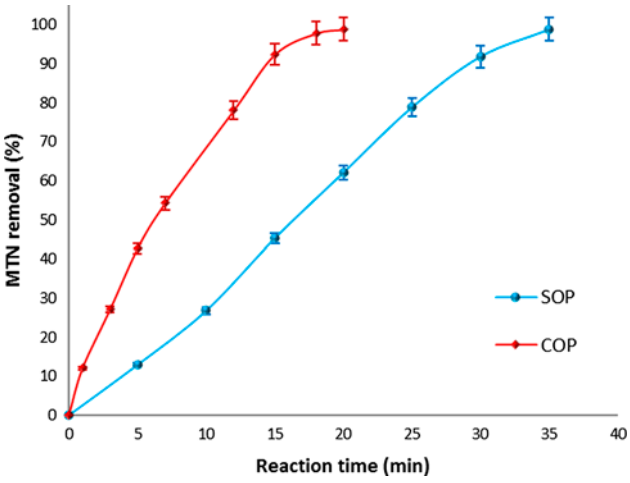

Fig. 4. Effect of reaction time on MNZ removal at: (a) the SOP (MNZ concentration = 40 mg/L, initial pH 10) and (b) the COP (MNZ concentration = 40 mg/L, initial pH 10, MgO dosage = 0.25 g/L).

results have been summarized in Table 2. According to these findings, MNZ degradation in both SOP and COP was best fitted with the pseudo-second-order model (linearized form type II), with a reaction constant of approximately 0.055 and 1.6 min^{-1}, respectively. Comparing the results indicates that the MgO nanocrystals with the ozonation process could accelerate the decomposition rate of MNZ. Hence, a higher rate of oxidation reaction and a shorter reaction time decrease the treatment costs. No previously published report could be found on the COP and SOP for MNZ removal for comparison with the results of the present work. The results presented here insinuate that due to high surface area and reactivity [17,18], simplicity of production, and destructive ability [19], the MgO nanocrystals are very promising catalysts for application in ozonation of MNZ-containing solutions.

3.4. Effect of MgO dosage

In order to invest catalyst dosage, the removal of MNZ was determined by the COP in the presence of various concentrations of MgO nanocrystals (ranging between 0.25 and 4 g/L). All experiments in this phase were carried out at the constant MNZ concentration of 40 mg/L, the optimum pH 10, and the reaction time of 15 min (at which the previous experiments showed 92% MNZ removal). MNZ removal variations as a function of catalyst concentration are shown in Fig. 5. According to Fig. 5, the MNZ removal increased from 45.2% in the absence of catalyst (SOP) to 92.4% in the presence of 0.25 g/L MgO nanocrystal powder. Afterward, it reached over 98% when the MgO dosage was increased to 3 g/L. A further increase in MgO dosage to 4 g/L did not increase the MNZ removal. Thus, due to the high surface area of MgO nanocrystals and an increase in the radical generation, small dosages of MgO nanocrystals are adequate to catalyze and raise the degradation of MNZ. The mechanisms were supposed to cause radical formation in the presence of ozone and MgO as shown below:

$$O_3 + (MgO - s) \rightarrow (MgO - s^{O_s}) \quad (2)$$

$$(MgO - s^{O_s}) \rightarrow (MgO - s^{O^\bullet}) + O_2 \quad (3)$$

$$(MgO - s^{O^\bullet}) + 2H_2O + O_3 \rightarrow (MgO - s^{\bullet OH}) + 3^\bullet OH + O_2 \quad (4)$$

Table 2
The results of kinetic models investigation by the linear regression method for degradation of MNZ by the SOP (MNZ concentration = 40 mg/L, initial pH 10) and the COP (MNZ concentration = 40 mg/L, initial pH 10, MgO dosage = 0.25 g/L)

	COP		SOP	
Kinetic models	R^2	Constant (min^{-1})	R^2	Constant (min^{-1})
Zero-order	0.9604	$k_0 = -0.00185$	0.9886	$k_0 = -0.0012$
First-order	0.8177	$k_1 = -0.0945$	0.8961	$k_1 = -0.0652$
Pseudo-first-order	0.9440	$k_{1p} = 0.2252$	0.8498	$k_{1p} = 0.1299$
Second-order	0.5731	$k_2 = -6.6$	0.7046	$k_2 = -4.7$
Pseudo-second-order				
Type (I)	0.9776	$k_{2p} = 0.9$	0.3353	$k_{2p} = 0.014$
Type (II)	0.9937	$k_{2p} = 1.6$	0.996	$k_{2p} = 0.055$
Type (III)	0.9247	$k_{2p} = 1.1$	0.3932	$k_{2p} = 0.12$
Type (IV)	0.9247	$k_{2p} = 0.94$	0.3932	$k_{2p} = 0.016$

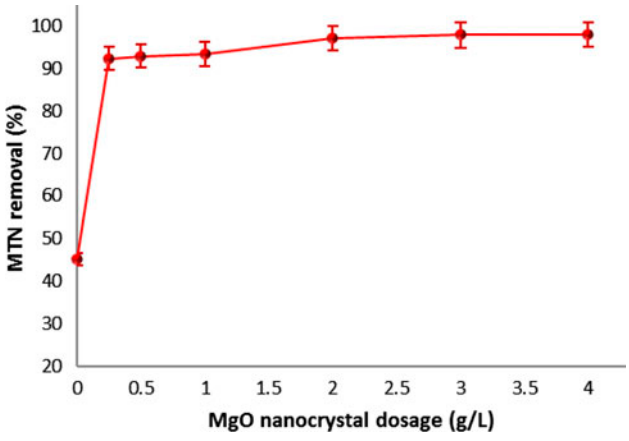

Fig. 5. Effect of MgO nanocrystals dosage on MNZ removal in the COP (MNZ concentration = 40 mg/L, initial pH 10, reaction time = 15 min).

As seen in Eqs. (2)–(4), the MgO nanocrystals act as an initiator for radical formation. Ozone is adsorbed on the surface of MgO and disintegrated into several active radicals. Indirect oxidation of MNZ molecules occurred because of all these radicals with higher rates than those seen with single ozone oxidation [39,40]. On the basis of these results and due to economic problems, 0.25 g/L was selected as the optimum dosage of MgO for the subsequent experiments. Moussavi et al. [15] added 5 g/L of MgO powder to the ozonation reactor in order to accelerate the oxidation efficiency of reactive red 198 dye.

The adsorption capacity of catalyst is one of the most important factors that can affect COP efficiency. In order to study the catalysts' adsorption capacity, 0.25 mg/L of MgO nanocrystals was added to 500 ml of the MNZ solution (MNZ concentration = 40 mg/L, initial pH 10) for 20 min of contact time without ozonation. The MNZ adsorption efficiency by the MgO nanocrystals under the optimum condition was determined to be less than 1%. This finding indicates that the main mechanism of MNZ degradation is reactions that are catalyzed by MgO nanocrystals and occurred on the surface of the catalyst.

3.5. Effect of initial MNZ concentration

Pharmaceutical wastewaters often contain different concentrations of antibiotics. Nevertheless, most of the COPs have been studied with a specific concentration of target contaminants. Hence, investigation of MNZ removal, as a function of the initial concentration of antibiotic, is very important. The effect of initial MNZ concentrations (1–40 mg/L) on MNZ removal in COP was investigated under the constant condition (initial pH 10 and a reaction time of 5 min). Fig. 6 depicts the removal of MNZ at various initial concentrations.

As shown in Fig. 6, removal efficiencies in COP for initial concentrations of 1, 5, 10, 20, 30, and 40 mg/L were 100, 90.6, 82.1, 52.8, 44.5, and 42.7%, respectively. These findings indicate that with an increase in the initial concentration of the antibiotic, the removal efficiency declined. This can be supplied by an increase in the ozone flow rate and/or ozonation time.

3.6. Biodegradability and mineralization

BOD_5/COD ratio usually indicates the wastewater biodegradability. A wastewater with BOD_5 to COD ratio of 0.4 or higher is considered easily biodegradable [15]. The biodegradability of raw and COP-treated MNZ solutions was investigated at a concentration of 40 mg/L of MNZ solution (selected concentration), which was 0.09 indicating that MNZ is a resistance compound. This ratio after passing the treatment in COP (under conditions of pH 10, MgO dose = 0.25 g/L, and reaction time = 20 min) increased to 0.43. These findings illustrate that the biodegradability of MNZ markedly ameliorated after a reaction time in COP and it was converted to a biodegradable waste. Farzadkia et al. [41] improved the biodegradability of MNZ solution from approximately 0 to 0.091 by nano-ZnO/UV photocatalytic process within 180 min.

TOC analysis showed that TOC of raw MNZ solution at 40 mg/L MNZ and COP effluent (under condition of pH 10, MgO dose = 0.25 g/L, and reaction time = 20 min) were 17 and 1.1 mg/L, respectively. These findings imply that the MNZ treatment with

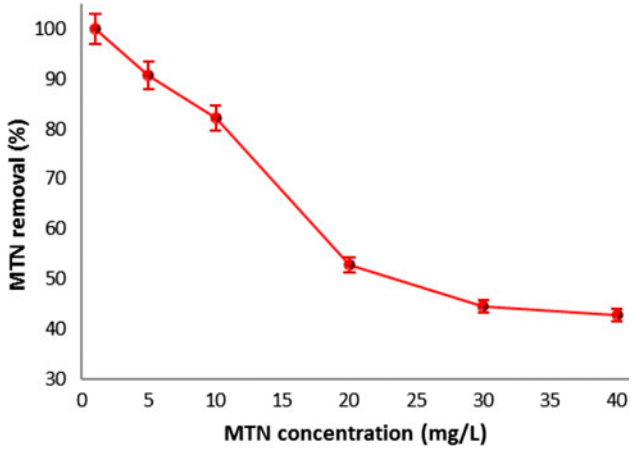

Fig. 6. Effect of initial MNZ concentration on MNZ removal in the COP (initial pH 10, reaction time = 5 min, MgO dosage = 0.25 g/L).

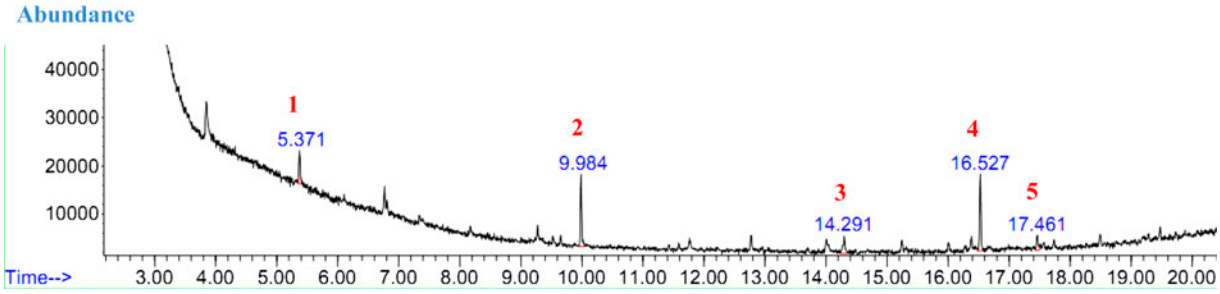

Fig. 7. MNZ oxidation intermediates after 10 min ozonation in COP (40 mg/L MNZ concentration, pH 10, 0.25 g/L MgO nanocrystal).

Table 3
Characteristics of oxidation intermediates

Peak number	Compound name	Chemical formula	Quality (%)	Molecular mass (g/mol)
1	Chloroform	$CHCL_3$	78	119.39
2	2,4 dimethyl Oxazole	C_5H_7NO	63	97.12
3	3-acetyl-2-oxazolidinone	$C_5H_7NO_3$	79	129.11
4	Dodecane	$C_{12}H_{26}$	94	170.33
5	1-Eicosanol	$C_{20}H_{42}O$	52	298.55

Table 4
Toxicity changes in influent and effluent of the COP

					Pearson goodness-of-fit test		
Solution	Remained MNZ (mg/L)	Time (h)	LC_{50} (% v:v)	TU[a]	χ^2	*df*	*p*-value
Influent	40	24	115.73	0.86	98.23	8	$p < 0.01$
Influent	40	48	80.76	1.24	143.69	8	$p < 0.01$
Effluent	n.d[b]	24	370.36	0.27	48.39	8	$p < 0.01$
Effluent	n.d	48	314.87	0.32	58.05	8	$p < 0.01$

[a]Toxicity unit.
[b]Non-detectable.

COP has a mineralization rate of about 93.5%. High mineralization reduces the environmental risks of effluent discharges.

3.7. Oxidation intermediates and effluent toxicity

All of the methods used for the degradation of contaminants will have some intermediates during the process and likely some byproducts at the end of the process. Sometimes these byproducts can be more dangerous than initial target contaminants. Fig. 7 shows the GC–MS chromatogram for intermediates' identification. According to Fig. 7, there are four intermediates for MNZ oxidation in COP. The first peak in the chromatogram is the solvent used for sample extraction. The characteristics of intermediates are shown in Table 3.

In order to invest toxicity changes in the COP, the LC_{50} of the effluent was determined after 24 h and 48 h by bioassay using D.Magna, under the optimum conditions (MNZ concentration = 40 mg/L, initial pH 10, MgO dosage = 0.25 g/L, and reaction time = 20 min) and compared with the bioassay results for the influent. The obtained desired concentrations were 0, 0.2, 0.4, 0.8, 2, 4, 8, 12, 20, 30, and 40 mg/L of MNZ. The results have been summarized in Table 4; the $TU\text{-}_{24h}$ and $TU\text{-}_{48h}$ for the influent of the COP decreased from 0.86 and 1.24 to 0.27 and 0.32 in the effluent, respectively. These findings indicate that longer contact time increased the MNZ toxicity and the COP with MgO

nanocrystals significantly reduced MNZ toxicity. Lanzky et.al also reported the acute toxicity of MNZ to freshwater and marine organisms [42].

4. Conclusions

The results of this study indicated that the COP by MgO nanocrystals can be applied as a complete or pre-treatment system for metronidazole-containing wastewaters. The optimum pH, MgO dosage, and required time for removal of 40 mg/L were 10, 0.25 g/L, and 20 min, respectively. Adding the MgO nanocrystals increased MNZ removal about 47% and decreased the required time compared to the conventional ozonation under the optimum condition. The COP had MNZ a mineralization rate of approximately 94% and significantly decreased the toxicity reducing the environmental risks of effluent discharges. Also, it improved the biodegradability of MNZ-containing solutions which makes it possible to be considered as post-treatment in a bioreactor.

Acknowledgment

The authors gratefully acknowledge the financial support of Iran University of Medical Sciences (IUMS); (Grant No: 21523).

References

[1] M.J. Ahmed, S.K. Theydan, Microporous activated carbon from Siris seed pods by microwave-induced KOH activation for metronidazole adsorption, J. Anal. Appl. Pyrolysis 99 (2013) 101–109.
[2] L.A. Dunn, A.G. Burgess, K.G. Krauer, L. Eckmann, P. Vanelle, M.D. Crozet, F.D. Gillin, P. Upcroft, J.A. Upcroft, A new-generation 5-nitroimidazole can induce highly metronidazole-resistant Giardia lamblia *in vitro*, Int. J. Antimicrob. Agents 36 (2010) 37–42.
[3] Y. Wang, P. Zhang, N. Jiang, X. Gong, L. Meng, D. Wang, N. Ou, H. Zhang, Simultaneous quantification of metronidazole, tinidazole, ornidazole and morinidazole in human saliva, J. Chromatogr. B 899 (2012) 27–30.
[4] Z. Fang, J. Chen, X. Qiu, X. Qiu, W. Cheng, L. Zhu, Effective removal of antibiotic metronidazole from water by nanoscale zero-valent iron particles, Desalination 268 (2011) 60–67.
[5] M.A. Hausen, R.F.S. Menna-Barreto, D.C. Lira, L. de Carvalho, H.S. Barbosa, Synergic effect of metronidazole and pyrantel pamoate on *Giardia lamblia*, Parasitol Int. 60 (2011) 54–58.
[6] J. Ré, M. De Méo, M. Laget, H. Guiraud, M. Castegnaro, P. Vanelle, G. Duménil, Evaluation of the genotoxic activity of metronidazole and dimetridazole in human lymphocytes by the comet assay, Mutat. Res. 375 (1997) 147–155.
[7] M.J. Ahmed, S.K. Theydan, Microwave assisted preparation of microporous activated carbon from Siris seed pods for adsorption of metronidazole antibiotic, Chem. Eng. J. 214 (2013) 310–318.
[8] H. Shemer, Y.K. Kunukcu, K.G. Linden, Degradation of the pharmaceutical Metronidazole via UV, Fenton and photo-Fenton processes, Chemosphere 63 (2006) 269–276.
[9] W. Cheng, M. Yang, Y. Xie, B. Liang, Z. Fang, E.P. Tsang, Enhancement of mineralization of metronidazole by the electro-Fenton process with a Ce/SnO_2–Sb coated titanium anode, Chem. Eng. J. 220 (2013) 214–220.
[10] M. Vertzoni, A. Carlsson, B. Abrahamsson, K. Goumas, C. Reppas, Degradation kinetics of metronidazole and olsalazine by bacteria in ascending colon and in feces of healthy adults, Int. J. Pharm. 413 (2011) 81–86.
[11] J. Rivera-Utrilla, G. Prados-Joya, M. Sánchez-Polo, M.A. Ferro-García, I. Bautista-Toledo, Removal of nitroimidazole antibiotics from aqueous solution by adsorption/bioadsorption on activated carbon, J. Hazard. Mater. 170 (2009) 298–305.
[12] R.F. Dantas, O. Rossiter, A.K.R. Teixeira, A.S.M. Simões, V.L. da Silva, Direct UV photolysis of propranolol and metronidazole in aqueous solution, Chem. Eng. J. 158 (2010) 143–147.
[13] W. Huiyan, Z. Gaoke, G. Yuanyuan, Photocatalytic degradation of metronidazole in aqueous solution by niobate $K_6Nb_{10.8}O_{30}$, Wuhan Univ. J. Nat. Sci. 15 (2010) 4.
[14] G. Moussavi, A. Khavanin, R. Alizadeh, The investigation of catalytic ozonation and integrated catalytic ozonation/biological processes for the removal of phenol from saline wastewaters, J. Hazard. Mater. 171 (2009) 175–181.
[15] G. Moussavi, M. Mahmoudi, Degradation and biodegradability improvement of the reactive red 198 azo dye using catalytic ozonation with MgO nanocrystals, Chem. Eng. J. 152 (2009) 1–7.
[16] K. He, Y.M. Dong, Z. Li, L. Yin, A.M. Zhang, Y.C. Zheng, Catalytic ozonation of phenol in water with natural brucite and magnesia, J. Hazard. Mater. 159 (2008) 587–592.
[17] R. Richards, R.S. Mulukutla, I. Mishakov, V. Chesnokov, A. Volodin, V. Zaikovski, N. Sun, K.J. Klabunde, Nanocrystalline ultra high surface area magnesium oxide as a selective base catalyst, Scr. Mater. 44 (2001) 1663–1666.
[18] F. Khairallah, A. Glisenti, Synthesis, characterization and reactivity study of nanoscale magnesium oxide, J. Mol. Catal. A: Chem. 274 (2007) 137–147.
[19] B. Nagappa, G.T. Chandrappa, Mesoporous nanocrystalline magnesium oxide for environmental remediation, Microporous Mesoporous Mater. 106 (2007) 212–218.
[20] G. Moussavi, A.A. Aghapour, K. Yaghmaeian, The degradation and mineralization of catechol using ozonation catalyzed with MgO/GAC composite in a fluidized bed reactor, Chem. Eng. J. 249 (2014) 302–310.

[21] APHA, Standard Methods for the Examination of Water and Wastewater, twentyfirst ed., American Public Health Association, Washington, DC, 2005.
[22] M.V. Lopez-Ramon, F. Stoeckli, C. Moreno-Castilla, F. Carrasco-Marin, On the characterization of acidic and basic surface sites on carbons by various techniques, Carbon 37 (1999) 1215–1221.
[23] USEPA, Methods for Measuring the Acute Toxicity of Effluents and Receiving Waters to Freshwater and Marine Organisms, fifth ed., US Environmental Protection Agency, Office of Water (4303T), Washington, DC, EPA-821-R-02-012, 2002.
[24] P.C.C. Faria, J.J.M. Órfão, M.F.R. Pereira, Activated carbon catalytic ozonation of oxamic and oxalic acids, Appl. Catal., B 79 (2008) 237–243.
[25] F. Erol, T.A. Özbelge, Catalytic ozonation with non-polar bonded alumina phases for treatment of aqueous dye solutions in a semi-batch reactor, Chem. Eng. J. 139 (2008) 272–283.
[26] U. von Gunten, Ozonation of drinking water: Part I. Oxidation kinetics and product formation, Water Res. 37 (2003) 1443–1467.
[27] B. De Witte, H. Van Langenhove, K. Demeestere, K. Saerens, P. De Wispelaere, J. Dewulf, Ciprofloxacin ozonation in hospital wastewater treatment plant effluent: Effect of pH and H_2O_2, Chemosphere 78 (2010) 1142–1147.
[28] B. De Witte, J. Dewulf, K. Demeestere, H. Van Langenhove, Ozonation and advanced oxidation by the peroxone process of ciprofloxacin in water, J. Hazard. Mater. 161 (2009) 701–708.
[29] B. Dewitte, J. Dewulf, K. Demeestere, V. Van De Vyvere, P. De Wispelaere, H. Van Langenhove, Ozonation of ciprofloxacin in water: HRMS identification of reaction products and pathways, Environ. Sci. Technol. 42 (2008) 4889–4895.
[30] M.C. Dodd, M.-O. Buffle, U. von Gunten, Oxidation of antibacterial molecules by aqueous ozone: Moiety-specific reaction kinetics and application to ozone-based wastewater treatment, Environ. Sci. Technol. 40 (2006) 1969–1977.
[31] R. Andreozzi, V. Caprio, A. Insola, R. Marotta, Advanced oxidation processes (AOP) for water purification and recovery, Catal. Today 53 (1999) 51–59.
[32] S. Esplugas, J. Giménez, S. Contreras, E. Pascual, M. Rodríguez, Comparison of different advanced oxidation processes for phenol degradation, Water Res. 36 (2002) 1034–1042.
[33] M. Sui, S. Xing, L. Sheng, S. Huang, H. Guo, Heterogeneous catalytic ozonation of ciprofloxacin in water with carbon nanotube supported manganese oxides as catalyst, J. Hazard. Mater. 227–228 (2012) 227–236.
[34] R. Joshi, S. Adhikari, B.S. Patro, S. Chattopadhyay, T. Mukherjee, Free radical scavenging behavior of folic acid: Evidence for possible antioxidant activity, Free Radical Biol. Med. 30 (2001) 1390–1399.
[35] Y.H. Dao, J. De Laat, Hydroxyl radical involvement in the decomposition of hydrogen peroxide by ferrous and ferric-nitrilotriacetate complexes at neutral pH, Water Res. 45 (2011) 3309–3317.
[36] J. Ma, N.J. Graham, Degradation of atrazine by manganese-catalysed ozonation—influence of radical scavengers, Water Res. 34 (2000) 3822–3828.
[37] J. De Laat, N. Boudiaf, F. Dossier-Berne, Effect of dissolved oxygen on the photodecomposition of monochloramine and dichloramine in aqueous solution by UV irradiation at 253.7 nm, Water Res. 44 (2010) 3261–3269.
[38] A. Behnamfard, M.M. Salarirad, Equilibrium and kinetic studies on free cyanide adsorption from aqueous solution by activated carbon, J. Hazard. Mater. 170 (2009) 127–133.
[39] B. Kasprzyk-Hordern, M. Ziółek, J. Nawrocki, Catalytic ozonation and methods of enhancing molecular ozone reactions in water treatment, Appl. Catal., B 46 (2003) 639–669.
[40] C.-H. Wu, C.-Y. Kuo, C.-L. Chang, Decolorization of C.I. Reactive Red 2 by catalytic ozonation processes, J. Hazard. Mater. 153 (2008) 1052–1058.
[41] M. Farzadkia, A. Esrafili, M.A. Baghapour, Y.D. Shahamat, N. Okhovat, Degradation of metronidazole in aqueous solution by nano-ZnO/UV photocatalytic process, Desalin. Water Treat. 52 (2014) 4947–4952.
[42] P.F. Lanzky, B. Halting-Sørensen, The toxic effect of the antibiotic metronidazole on aquatic organisms, Chemosphere 35 (1997) 2553–2561.